

WL-TR-95-4098

RELATIONSHIP OF THE SECOND ORDER
NONLINEAR OPTICAL COEFFICIENT TO BANDGAP IN



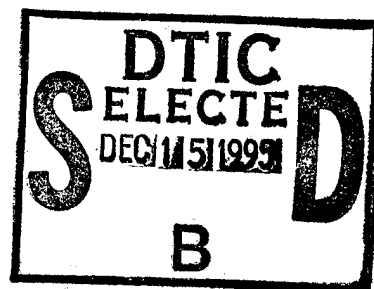
A.G. JACKSON
M. OHMER
S.R. LECLAIR

TMCI
P.O. BOX 340345
BEAVERCREEK OH 45434-0345

MAY 1995

FINAL REPORT FOR 01/01/94-01/01/95

APPROVED FOR PUBLIC RELEASE; DISTRIBUTION IS UNLIMITED.



19951214 067


MATERIALS DIRECTORATE
WRIGHT LABORATORY
AIR FORCE MATERIEL COMMAND
WRIGHT PATTERSON AFB OH 45433-7734

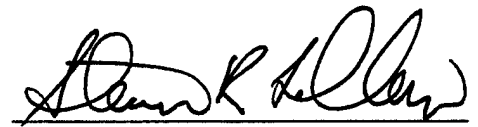
NOTICE


When Government drawings, specifications, or other data are used for any purpose other than in connection with a definitely Government-related procurement, the United States Government incurs no responsibility or any obligation whatsoever. The fact that the Government may have formulated or in any way supplied the said drawings, specifications, or other data, is not to be regarded by implication, or otherwise in any manner construed, as licensing the holder, or any other person or corporation; or as conveying any rights or permission to manufacture, use, or sell any patented invention that may in any way be related thereto.

This report is releasable to the National Technical Information Service (NTIS). At NTIS, it will be available to the general public, including foreign nations.

This technical report has been reviewed and is approved for publication.


STEVEN R. LECLAIR, Chief
Materials Process Design
Integration & Operations Division
Materials Directorate


STEVEN R. LECLAIR, Chief
Materials Process Design
Integration & Operations Division
Materials Directorate


JOHN R. WILLIAMSON
Integration & Operations Division
Materials Directorate

If your address has changed, if you wish to be removed from our mailing list, or if the addressee is no longer employed by your organization please notify WL/MLIM, Wright Patterson AFB, OH 45433 to help maintain a current mailing list.

Copies of this report should not be returned unless return is required by security considerations, contractual obligations, or notice on a specific document.

REPORT DOCUMENTATION PAGE

Form Approved
OMB No. 0704-0188

Public reporting burden for this collection of information is estimated to average 1 hour per response, including the time for reviewing instructions, searching existing data sources, gathering and maintaining the data needed, and completing and reviewing the collection of information. Send comments regarding this burden estimate or any other aspect of this collection of information, including suggestions for reducing this burden, to Washington Headquarters Services, Directorate for Information Operations and Reports, 1215 Jefferson Davis Highway, Suite 1204, Arlington, VA 22202-4302, and to the Office of Management and Budget, Paperwork Reduction Project (0704-0188), Washington, DC 20503.

1. AGENCY USE ONLY (Leave blank)	2. REPORT DATE MAY 1995	3. REPORT TYPE AND DATES COVERED FINAL 01/01/94--01/01/95
----------------------------------	----------------------------	--

4. TITLE AND SUBTITLE RELATIONSHIP OF THE SECOND ORDER NONLINEAR OPTICAL COEFFICIENT TO BANDGAP IN IN INORGANIC NON-CENTROSYMMETRIC CRYSTALS	5. FUNDING NUMBERS C F33615-94-D-5801 PE 62102 PR 2418 TA 90 WU 01
---	---

6. AUTHOR(S)
A. G. JACKSON
M. OHMER
S. R. LECLAIR

7. PERFORMING ORGANIZATION NAME(S) AND ADDRESS(ES)
TMC I
P.O. BOX 340345
BEAVERCREEK OH 45434-0345

8. PERFORMING ORGANIZATION
REPORT NUMBER

9. SPONSORING/MONITORING AGENCY NAME(S) AND ADDRESS(ES)
MATERIALS DIRECTORATE
WRIGHT LABORATORY
AIR FORCE MATERIEL COMMAND
WRIGHT PATTERSON AFB OH 45433-7734

10. SPONSORING/MONITORING
AGENCY REPORT NUMBER
WL-TR-95-4098

11. SUPPLEMENTARY NOTES

12a. DISTRIBUTION/AVAILABILITY STATEMENT
APPROVED FOR PUBLIC RELEASE; DISTRIBUTION IS
UNLIMITED.

12b. DISTRIBUTION CODE

13. ABSTRACT (Maximum 200 words)

Second order nonlinear optical coefficient data and band gap data collected from the literature have been classified and are organized by plotting their respective values. The two-dimensional plots indicate that both large bandgap - and small $X(2)$, and small bandgap - and large $X(2)$ are highly correlated. A corresponding trend is also demonstrated for the figure of merit which is used to rank materials for wavelength conversion efficiency. Results of the analysis are used to estimate the second order nonlinear optical properties and conversion efficiencies of several less-well-known materials. Trend analysis suggests that ordered GaInP_2 would be exceptional as a E-O waveguide material and that the FOM of AgGaTe_2 is 3.6 times that of AgGaSe_2 and that crystals of HgGa_2Se_4 and $\text{Te}_x\text{Se}_{(1-x)}$ alloys should be of distinct interest as wavelength conversion materials for infrared applications. The maximum attainable $X(2)$ is in the range of 3500-4000 pm/V for bound electrons. For bandgaps less than one eV, the increase in $X(2)$ with decreasing bandgap slows considerably.

DTIC QUALITY INSPECTED 2

14. SUBJECT TERMS
nonlinear optical properties, crystal, bandgap

15. NUMBER OF PAGES
30

16. PRICE CODE

17. SECURITY CLASSIFICATION
OF REPORT
UNCLASSIFIED

18. SECURITY CLASSIFICATION
OF THIS PAGE
UNCLASSIFIED

19. SECURITY CLASSIFICATION
OF ABSTRACT
UNCLASSIFIED

20. LIMITATION OF ABSTRACT
SAR

INTRODUCTION

The purpose of this paper, is to provide a means of estimating and comparing the wavelength conversion efficiency (figure of merit, FOM) of new nonlinear materials knowing only their bandgap. The approach for the estimates is trend analysis of existing data¹⁻²⁸ for the second order nonlinear coefficient, $\chi^{(2)}_{ijk}$, or $d_{ij} = \chi^{(2)}_{ijk}/2$, the index of refraction n , and the bandgap E . No underlying physical basis for the result will be presented. The result of this trend analysis, in the form of plots of $\chi^{(2)}$ vs E and FOM vs E and the associated fit equations, will be used to estimate $\chi^{(2)}$ and the FOM for wavelength conversion efficiency for some new materials. The accuracy goal agrees within a factor of 2-5 with the experimental values, which is quite good considering the values range over four to seven orders of magnitude.

In this paper, following the usual conventions, the $\chi^{(2)}$ values are treated as having constant values in the region of high transparency between the bandgap and the onset of multiphonon absorption, and the full $\chi^{(2)}$ values are used, which means the impact of the phase matching angle is ignored. The requirement to phase match often reduces significantly the effective $\chi^{(2)}$ values below those of the full values. The distinction between direct, indirect, or pseudodirect bandgaps is ignored and the minimum room temperature gap is used in all cases.

A number of trends are now well known for semiconductors. Representative examples are: a decreasing thermal conductivity as the bandgap decreases, an increasing mobility as the bandgap decreases, an increasing spin-orbit splitting as the bandgap decreases, a decreasing bandgap as the lattice constant increases, an increasing index of refraction as bandgap decreases, an increasing dielectric constant as bandgap decreases, and increasing non-linear susceptibilities as the linear susceptibilities increase. The last three examples are relevant to the present discussion and will be described in some detail below, followed by some observations related to corresponding *ab initio* calculations.

The nonlinear optical behavior of crystals in response to intense optical beams is understood in

for	
<input checked="checked" type="checkbox"/>	
<input type="checkbox"/>	
<input type="checkbox"/>	
on	
by Codes	
Dist	Avail and/or Special
A-1	

terms of a nonlinear polarization^{11,28}. The polarization tensor $P(E)$ is related to the electric field tensor E through Eq (1) or Eq (2), where, $\chi^{(2)}_{ij} = 2 d_{ij}$, κ is the dielectric susceptibility, $\chi^{(2)}$ (subscripts are omitted subsequently) and $\chi^{(3)}$ are the nonlinear susceptibility coefficients.

$$P(E) = \kappa(E) \cdot E = \kappa_0 E + \chi^{(2)} \cdot E^2 + \chi^{(3)} \cdot E^3 + \dots \quad (1)$$

$$P_i = \kappa_{0ik} E_k + \chi^{(2)}_{ij} E_j^2 + \dots, \quad (2)$$

In Eq (2), the three dimensional tensor is written in the usual "plane" representation. In the following discussion, the subscripts will be omitted except where helpful for clarity of meaning. All non-centrosymmetric compound semiconductors will have a non-zero $\chi^{(2)}$ and be optically transparent. Generally speaking for infrared applications, all III-V and II-VI compound semiconductors and their pseudo-ternary analogs, the I-III-VI₂ and II-IV-V₂ chalcopyrites with bandgaps of the order of 2 eV or less, have large $\chi^{(2)}$'s. A number of compounds from these families with $\chi^{(2)}$'s in the range of 66 pm/V (i.e., AgGaSe₂) to the enormous value of 470 pm/V (i.e., CdGeAs₂) have received serious consideration for infrared applications.

The usual FOM for wavelength conversion efficiency can be expressed as $(\chi^{(2)})^2/n^3$, where χ is the effective χ -value which depends on the specific crystal structure and the direction of the incident optical beam on the crystal and n is the index of refraction in the transparent region. For the zinc blende or the chalcopyrite semiconductors the appropriate χ is χ_{36} . It is traditional to compare $\chi^{(2)}$ values only and ignore the issue of beam direction in first order comparisons of the nonlinear optical properties. In this paper trend analysis of $\chi^{(2)}$ vs bandgap and FOM vs bandgap is used to estimate the size of $\chi^{(2)}$ and the FOM for wavelength conversion efficiency for known and unknown materials.

A trend between index of refraction and bandgap was pointed out by Moss²⁷ in 1950. The

Moss expression for the index of refraction n , where the constant has been slightly modified by Ravindra and Srivastava²⁶, is given as Eq (3), where the energy in this and subsequent equations is in eV:

$$n = (108/E)^{1/4} \quad (3)$$

The data compiled and modeled by Phillips²⁹ and VanVechten³⁰ presented a corresponding relationship between the dielectric constant ϵ or linear susceptibility $\chi^{(1)}$ and energy gap, as pointed out by Soref³¹, as the Moss-like relationships of Eqs (4) and (5).

$$\epsilon = (a/E)^{1/2} \quad (4)$$

or

$$\chi^{(1)} = (b/E)^{1/2} \quad (5)$$

where a and b are appropriate constants. Considering that $n^2 = \epsilon$, Eq (4) has the same functional form as Eq (3). The physical basis for Eq (4), Eq (5), and by inference Eq (3), is provided within the framework of the Phillips' bond charge model^{29,30}.

Miller³² in 1964 noticed that the $\chi^{(2)}$ values available for eleven materials could vary by several orders of magnitude from material to material. He found to his surprise that the $\chi^{(2)}$ is proportional to a product of the three linear susceptibilities. This relationship is now known as Miller's Empirical Rule and the proportionality constant is known as Miller's δ_{ij} . Flytzanis³³ states that, in a certain sense, this rule was the first hint that nonlinear susceptibilities could be expressed in terms of other macroscopic properties. If the mean value of δ_{ij} determined for these 11 materials is used, then all of the d values can be calculated to within a factor of two. The rule can also be written in terms of indices or dielectric constants. For indices the rule can be written³¹ in rationalized mks

units:

$$\chi^{(2)} = 2(8.85 \times 10^{-12}) (n_{\omega}^2 - 1)^2 (n_{2\omega}^2 - 1) \delta_{ij}, \quad (6)$$

where $\chi^{(2)}$ is in m/V and n_{ω} and $n_{2\omega}$ are the indices respectively at the frequencies ω and 2ω . Miller's original constant value for δ_{ij} in his units was 0.38 and the specific value for GaAs was 0.24. Using the presently accepted value of 180 pm/V for χ_{36} gives a value for Miller's delta of 0.0246 in rationalized mks units, which yields

$$\chi^{(2)} = 0.436 (n_{\omega}^2 - 1)^2 (n_{2\omega}^2 - 1), \quad (7)$$

where the units of $\chi^{(2)}$ are pm/V.

Subsequently, Flytzanis and Ducuing³⁴, in a study of the specific material-to-material variation of δ_{ij} within the III-V semiconductor family, found that Miller's delta correlates remarkably well with the dipole moment of the cation-anion bond. Ultimately, using the bond charge model, Levine³⁵ provided an approach for calculating the value of δ_{ij} for a given material. Levine's value for δ_{ij} used in conjunction with Miller's Empirical Rule overestimates the experimental values by 20% or less for a large number of semiconductors. This modification based on physical insight greatly improved the accuracy of Miller's Empirical Rule. However, it was Miller's Empirical Rule that provided the insight for the establishment of the underlying physical basis for nonlinear optical susceptibility .

Ignoring dispersion, Miller's Empirical Rule, as given by Eq 7, reduces approximately, for large index materials, for $n^2 \gg 1$, to :

$$\chi^{(2)} = (0.436) n^6 (\delta_{ij}), \quad (8)$$

Combining Miller's rule, Eq (6), and the Moss relationship, Eq (3), indicates that for $\chi^{(2)}_{ij}$ increases rapidly as E decreases, going as $(1/E)^{3/2}$. In the same spirit, the FOM also increases rapidly as E decreases, going as $(1/E)^{9/4}$. Tabulations of $\chi^{(2)}$ values versus transparency range given by Prokhorov³⁷, or of the FOM for wavelength conversion versus transparency range given by Shay and Wernick³⁸ for representative materials, also suggest the trend that nonlinear properties increase rapidly with decreasing bandgap. The prior successes of empirical property trend analysis have served as the motivation for the FOM trend analysis to follow.

The alternate approach of *ab initio* calculations of the corresponding quantities, particularly for even-order susceptibilities like $\chi^{(2)}$, is presently not generally feasible. Flytzanis³³ has reviewed efforts to produce approximate theoretical scaling laws for nonlinear susceptibilities and Levine et al.³⁹ and Zhong et al.⁴⁰ have made "near" *ab initio* calculations of the nonlinear susceptibilities. These two approaches are discussed below.

Flytzanis has shown that odd order nonlinear susceptibilities, like the linear one can be cast in the form of scaling laws, essentially power laws of an effective parameter which turns out to be a measure of the valence electron delocalization and can be expressed in terms of measurable macroscopic quantities. It is found that for three-dimensional systems the odd order susceptibilities scale as:

$$\chi^{(2m-1)} = (P^2)(1/E^{(3m-1)}), \quad (9)$$

where P is the average transition-dipole-moment matrix element and $m = 0, 1, 2, \dots$. For $\chi^{(1)}$ and $\chi^{(3)}$ Eq (9) gives

$$\chi^{(1)} = P^2/E^2 \quad (m = 1) \quad (10)$$

and

$$\chi^{(3)} = (P^2)(1/E^5). \quad (m = 2) \quad (11)$$

Note that the ratio of $\chi^{(1)}$ to $\chi^{(3)}$ yields $\chi^{(3)} = \chi^{(1)}/E^3$. Eq (10) may be compared to Eq (5), implying that P^2 scales as $E^{-3/2}$, for $\chi^{(1)}$ scaling as $E^{-1/2}$, and that $\chi^{(3)}$ scales as in Eq (12) below:

$$\chi^{(3)} = (c)(1/E)^{6.5}, \quad (12)$$

where c is an appropriate constant. These scaling laws were derived in the one-electron approach, ignoring electron correlations via a critical point analysis. These scaling laws might become invalid as the average atomic number of the compound increases to the point that spin-orbit-splitting is a significant portion of the gap. This occurs for very narrow gap materials.

Sheik-Bahae et al.³⁶ used a two band model to calculate the scaling of $\chi^{(1)}$ and found that empirically an E^{-4} dependence is successful in predicting the $\chi^{(3)}$ for a wide variety of semiconductors and insulators over four orders of magnitude. This is a somewhat slower but similar dependence to the $E^{-6.5}$ dependence given by Eq (12).

It is not possible³³ to provide a similar approximate theoretical expression for even-order susceptibilities such as $\chi^{(2)}$ because it is sensitive to local properties of the electron density, and integration over the entire Brillouin Zone is required. The physical basis is that the simultaneous requirement for large charge asymmetry and large charge delocalization are competing processes resulting in some cancellation effects. However, the empirical trend for $\chi^{(2)}$ and the approximate theoretical scaling laws for odd order susceptibilities indicate that, generally, susceptibilities are a power law function of the bandgap, increasing rapidly as the bandgap decreases.

The "nearly" *ab initio* calculations of the nonlinear susceptibilities for some III-V compounds and Se have been reported^{37,38}. At present *ab initio* calculations do not accurately predict the bandgap, tending to produce a value about 1.0 eV too small and a lattice constant 0.100 to 0.200 nanometers too small. Unfortunately, the value of $\chi^{(2)}$ is extremely sensitive to lattice

constant/bond length and bandgap³⁷. These limitations are overcome by adding a constant self-energy correction to the Hamiltonian to fix the bandgap and using the experimental lattice parameters. This "nearly" *ab initio* approach then gives good agreement with experimental results for compounds of elements in and above Period IV. However, for elements and compounds in Period V or greater such as Te, CdGeAs₂, and InSb, this approach does not apply, as once again spin-orbit-splitting has not yet been taken into account. The results for the five materials for which $\chi^{(2)}$ was calculated also shows the general trend that $\chi^{(2)}$ increases rapidly with decreasing bandgap. Fitting the data indicates that $\chi^{(2)}$ increases as E^{-3} and FOM as E^{-6} .

Flytzanis³³ points out that the searches for scaling laws and empirical trend analysis for susceptibilities, as for other physical properties, serves many purposes, fundamental as well as practical. They allow the prediction of the properties of new materials by simple inspection, they introduce economy in comparing materials, and they help formulate guidelines for the search for new materials, as well as provide guidance for the development of theory by singling out dominant mechanisms. In the general case, scaling laws and empirical trend analysis are the only tools available for guiding new materials development.

RESULTS AND DISCUSSION

Using a database compiled from the literature for a number of compounds of interest for nonlinear optical applications, a plot of the second order nonlinear coefficient, $\chi^{(2)}$, versus bandgap has been constructed, and is given in Figure 1. A similar plot of the FOM versus bandgap is given in Figure 2. Where known or observed, uncertainty for these values was noted; otherwise a minimum of $\pm 20\%$ relative error was assumed, a value most likely too small an error for much of the data in view of the wide variability observed from the literature where some error ranges approach factors of two. In converting from relative to absolute values the value of $\chi^{(2)}_{36} = 180$ pm/V from reference 14 has been used following general practice. We note that many values

reported in the literature have been converted using much higher values ranging from 139 to 151, which give values larger by 50% to 70%. In Table 1, Soref's $\chi^{(2)}$ values for IV-IV compounds are used. These are calculated values assuming Miller's rule and using δ_{ij} for SiC. This approach, in view of the saturation shown in Figure 1, may overestimate significantly the $\chi^{(2)}$'s of the narrow bandgap members of the family such as GeSn.

The general trend of both $\chi^{(2)}$ and FOM is to increase rapidly with decreasing bandgap. In Table 1 are listed the data (and sources) used in the plots. Examination of the curves shows that a single power law expression cannot represent the data well over the total bandgap range. Regression fits were computed which relate $\chi^{(2)}$ to bandgap and FOM to bandgap for a single curve over the full range of E, and two curves. The least squares fits are listed in Table 2. A power law was chosen because it is consistent with the results of the ones discussed in the introduction, although $\chi^{(2)}$ also can be fit reasonably well an e^{-E} type law ($\chi^{(2)} = 1134e^{-1.1E}$). Clearly, the single curve overestimates large band gap compounds, while underestimating small band gap compounds. For those materials with gaps from about 0.8 to about 3 eV, the single curve fit provides an order of magnitude estimate. The two curves provide better estimates for the ranges 0 to about 1 eV and 1 to about 8 eV. We note that the Miller's δ values are rather widespread for this set of compounds, covering a range of about a factor of two, and having an average value of about $0.05 \text{ m}^2/\text{C}$.

Calculated values based on Table 2 and actual values are listed in Table 3 for several well known materials. Table 3 indicates that predictions are within a factor of two in the IR for both $\chi^{(2)}$ and FOM, and over the full range all agree approximately within the goal of a factor of 2-5. Further comparisons are presented in Tables 4 and 5. In Table 4, predicted values and actual values for families are compared by calculating ratios for three groupings, using the lowest value of the group as a reference. The results are presented in columns 5 and 6, and they suggest that the predicted values are close to the actual values where known. Again the accuracy is within a factor of two in the IR. In Table 5 a similar comparison is made for FOM. The results indicate reasonable agreement except for the narrow band, where the predicted value severely underestimates the actual

value, although the agreement with the relative value is within a factor of two. Also, we note that predicted values of FOM may be in error by factors more than two, because $\chi^{(2)}$ enters FOM as the square. The trend, however, is valid for FOM.

The fits in Table 2 are applied to four promising relatively unknown materials; 1) the recently discovered ordered ternary III-V compound GaInP₂, predicted by Wei and Zunger⁴¹ for which no nonlinear properties are available, 2) the less well known AgGaTe₂ whose nonlinear properties have not been reported and which is a member of the compound family whose two well known members are AgGaS₂ and AgGaSe₂, 3) several new members of the II-III₂-VI₄ family, defect or pseudo chalcopyrites, which includes the well known mercury thiogallate, HgGa₂S₄, and 4) TeSe solid solution alloys which have not received the consideration they deserve as very high efficiency materials. These Equations are also applied to three well known materials, GaAs, ZnGeP₂ and CdGeAs₂ as baseline comparisons. All of these results are presented in Table 5. As a final discussion, several additional subtrends based on families of compounds are discussed.

Random ternary alloy III-V semiconductors have received little attention, although their $\chi^{(2)}$ s can be very large, because they are isotropic, and, therefore, do not possess birefringence which is necessary for conventional wavelength conversion processes. However, in the ordered state it would be expected that ternaries like GaInP₂ would be birefringent uniaxial crystals. Stenger et al.⁴² have experimentally verified this expectation of adequate birefringence by variable angle spectral ellipsometry measurements for CuPt-like ordering in GaInP₂. The estimated $\chi^{(2)}$ from Table 4 for ordered GaInP₂ is 130 pm/V, a value large in practical terms. This seems to be a very reasonable value, since it is somewhat less than the trend value for GaAs of 214 pm/V, as would be expected from its slightly larger bandgap, and the trend result for GaAs is in fairly good agreement with the literature¹⁹ value of 180 pm/V. It would seem that films of ordered GaInP₂ would be exceptional waveguide materials.

Some years ago, Bell et al.⁴³ investigated the properties of the AgGaTe₂ compounds and commented that AgGaTe₂ had good mechanical properties and should have a sufficiently large birefringence to be useful for nonlinear optics, although there had not been any studies of this

aspect of the AgGaTe₂ compounds. Because $\chi^{(2)}$ data for AgGaTe₂ is not available from the literature, the estimated value from Table 4 is 233 pm/V. Comparing trend results with literature values for AgGaS₂ and AgGaSe₂ indicates that, for this family, the trend result overestimates the literature values but does accurately reflect the relative values for these two materials as shown in column VII of Table 4. In Figure (1), the II-VI compounds and their pseudo-ternaries lie generally lower while following the same slope which is consistent with the actual materials dependence of Miller's δ . Relying on the more reliable relative value would give a $\chi^{(2)}$ of 101 pm/V which exceeds the value for AgGaSe₂ by 60% and more importantly a factor of 3.5 times greater FOM. This material is certainly worth re-exploring.

Radautsan et al.⁴⁴ have surveyed a number of the II-III₂-VI₄ compounds and indicate that their nonlinear properties are interesting. The thiogallates HgGa₂S₄, HgGa₂Se₄, HgIn₂Se₄ are compared using Table 2 and the bandgaps reported by Radautsan et al. The trend result of 36.2 pm/V for $\chi^{(2)}$ for HgGa₂S₄ is in reasonable agreement with the literature value¹¹ for $\chi^{(2)}$ which ranges from 53.6 pm/V to 70.4 pm/V. So the trend results listed in Table (3) should be reasonable estimates. For HgIn₂Se₄, the estimate for $\chi^{(2)}$ is an impressive 196 pm/V, its FOM is a factor of 15 larger than that of HgGaS₄! Its range of transparency should be quite large, given its calculated range is from 0.86 microns to much greater than 12 microns, the long-wavelength cut-off of HgGa₂S₄.

Tellurium has the second highest reported $\chi^{(2)}$ for a semiconductor and it is transparent in the infrared. However, in CO₂ laser doubling experiments it has been found that two photon absorption and intraband scattering of free carriers limits its application to low power levels. This is a result of its narrow bandgap. This problem could be alleviated by alloying with Se to increase the bandgap. Pure tellurium crystals are quite soft and deformation induced defects also limit its performance⁴⁵. Alloy hardening may adequately improve its mechanical properties. The optical properties of Te crystals alloyed with respectively 2%, 2.7%, and 11% have been reported^{46,47}. There is evidence that a solid solution exists for all concentrations⁴⁶ where the lattice constant decreases in a linear fashion as selenium is added to tellurium. The bandgaps in eV and the

respective short wavelength cut-offs in microns for the 0%, 2.7%, 11%, and 100% cases are respectively 0.358/3.46, 0.375/3.3, approximately 0.4/3.1, and 1.7/0.72. Alloying provides a method of continuously varying the cut-off from 3.46 to .72 microns. The $\chi^{(2)}$ and the FOM will vary with composition as the bandgap varies as indicated by Eq (4) and (5), but this dependence may be nonlinear, as pointed out by Stuke and Keller⁴⁸. Thus, a linear interpolation of band gap values from pure Te and pure Se based on composition will yield incorrect results. Using the bandgap composition results of Stuke and Keller, for a 1 eV bandgap/1.24 micron cut-off alloy, the composition $\text{Te}_{.286}\text{Se}_{.714}$ is required. Once a bandgap value is estimated, $\chi^{(2)}$ and FOM can be read from the plots; in this case, this compound has a $\chi^{(2)}$ of about 700 pm/V and FOM of about 3000 pm²/V².

The intraband scattering mechanism mentioned above which limits the performance of Te will be much less severe in the alloys. As the bandgap is widened the valence band splitting is significantly smaller in comparison, and this scattering mechanism is much less important. In addition, Dubinskaya⁴⁶ reports an approach which may overcome this limitation. Te and, by analogy, these alloys are easily bleached to improve their transparency in the infrared by exposing the crystals to weak visible light sources. The impressively large values for the nonlinear parameters indicate that a serious exploration of this alloy system is warranted.

The power law dependencies for FOM and $\chi^{(2)}$ are summarized in Table 6 and discussed below. Empirically, the FOM depends more strongly on E than $\chi^{(2)}$ does. As a result, reducing the bandgap is significantly more beneficial than the $\chi^{(2)}$ trend alone might indicate. From the fit for $\chi^{(2)}$ in the bandgap range > 1 eV, and from the "nearly" *ab initio* calculation for the 1.4 - 2.45 eV range, the bandgap dependences are similar, as $m = 2.6$ and 3, respectively. For the FOM the "nearly" *ab initio* result and our results give respectively $m = 6$ and $m = 4.1$ (using our large gap value) or $m = 0.9$ using our small gap value, indicating that the field dependence of FOM is overestimated by the calculated results.

For bandgaps <1 eV, the bandgap dependence for both FOM and $\chi^{(2)}$ are strikingly lower as saturation sets in. A comparison of "nearly" *ab initio* results for the narrow bandgap materials has

not been made, because the model does not include spin-orbit-splitting and it is useful only for compounds made up of low atomic number atoms⁴⁹. The bond charge model, the approximate *ab initio* model, and the "nearly" *ab initio* model fail to predict the saturation observed for FOM and $\chi^{(2)}$, although Miller's rule does, as shown in Figure 1. However, Miller's rule does poorly in the wide bandgap regime, tending to overestimate significantly. At the present time the bandgap dependence over the full range is treated successfully only by trend analysis, which covers materials with a gap of less than one eV.

A more careful look at the trends in Fig. (1) indicates that the data can be grouped in a number of ways to identify sub-trends. Compounds with Group V or VI anions can be grouped as the upper or high bandgap group while oxides and complex structures as the lower or low bandgap group. Using these groupings, there are at least two curves present -- one for narrow bandgap and one for large bandgap. Several compound families show similar slopes when the anion element is considered, for example, {ZnS, ZnSe, ZnTe}, {CdS, CdSe, CdTe}, {GaP, GaAs, GaSb}, {CuGaS₂, CuGaSe₂}, {Se, Te} and {AgGaS₂, AgGaSe₂} have similar slopes. The sulfides and the selenides tend to fall below the trend line, for the III-V compounds, in agreement with their smaller Miller's δ 's. The II-IV-V₂ family members, on the other hand, tend to fall above the trend line for the III-V compounds, in agreement with their large Miller's δ 's. The {CdGeP₂, CdGeAs₂} line has a lower slope than the others, as does {ZnS, CdS, HgS}. The {InP, InAs, InSb} trio does not lie on a line, suggesting that the data may be suspect, probably for the InAs, because the line for InP and InSb has a slope similar to that for similar groupings. The predicted value for In As is about 1650 pm/V \pm 500. If the {CdGeP₂, CdGeAs₂} data is correct, this suggests that the $\chi^{(2)}$ value for ZnGeAs₂ should be about 356 pm/V \pm 75 based on the direct bandgap value of about 1.15 eV. However, it is anticipated that ZnGeAs₂ will not possess an adequate birefringence, because its tetragonal distortion is zero (i.e., $c/a = 2.0$).

CONCLUSIONS

As a means for quickly estimating the value of a material, these curves offer a simple and direct means for classifying nonlinear optical materials. The plots show a strong trend in the data, i.e., $\chi^{(2)}$ increasing rapidly with decreasing bandgap. The FOM depends more strongly on E than $\chi^{(2)}$ does, and, as a result, reducing the bandgap is significantly more beneficial than the $\chi^{(2)}$ trend alone might indicate. The bandgap dependence of the "nearly" *ab initio* and that of our empirical result for the bandgap near and above one eV are identical. A saturation of $\chi^{(2)}$ at band gaps below one eV is observed in our empirical trend, although the various models described fail to predict this behavior, and trend analysis is superior to Miller's rule for large bandgaps. This relationship alone is of value in estimating $\chi^{(2)}$ for a compound based on band gap value. Thus, a non-centrosymmetric compound can be evaluated in broad terms as to its utility as a $\chi^{(2)}$ nonlinear optical material. Trend analysis indicates that films of ordered GaInP₂ would be exceptional as E-O waveguide materials, that the FOM of AgGaTe₂ is an impressive factor of 3.5 times greater than that of AgGaSe₂ and crystals of HgGa₂Se₄, and that Te_xSe(1-x) alloys are of distinct interest, because they are very efficient wavelength conversion materials for infrared application.

ACKNOWLEDGMENT

AGJ gratefully acknowledges the support provided by AF contract F33615-90-5944 with Wright Laboratory.

REFERENCES

1. J. E. Jaffe and A. Zunger, *Phys. Rev. B* **28**, 5822 (1983).
2. J. C. Rife, R. N. Dexter, P. M. Bridenbaugh, and B. W. Veal, *Phys. Rev. B* **16**, 4491 (1977).
3. A. Heinrich, W. Cordts, and J. Monecke, *Phys. Status Solidi B* **107**, 319 (1981).
4. J. E. Jaffe and A. Zunger, *Phys. Rev. B* **27**, 5176 (1983).
5. Alex Zunger, *Phys. Rev. B* **22**, 5839 (1980).
6. Alex Zunger and J. E. Jaffe, *Phys. Rev. Lett.* **51**, 662 (1983).
7. S. H. Wei and Alex Zunger, *Appl. Phys. Lett.* **56**, 662 (1990).
8. A. Sileika, *Inst. Phys. Conf. Ser.* **35**, 129 (1977).
9. A. S. Poplavnoi, Y. I. Polygalov, and A. M. Ratner, *Izv. Vyssh. Uchebn. Zaved, Fiz.* [Sov. Phys. J.] **19**, 7 (1976).
10. H. Horinaka, and N. Yamamoto, *Oyo Butsuri* **60**, 112 (1991).
11. V. G. Dmitriev, G. G. Gurzadyan, and D. N. Nikogosyan, *Handbook of Nonlinear Optical Crystals*, Springer Series in Optical Sciences, Vol. 64, Springer-Verlag Berlin Heidelberg, 1991.
12. R. Poerschke and O. Madelung, *Semiconductors - Other than Group IV Elements and III-V Compounds*, Data in Science and Technology, Springer-Verlag Berlin Heidelberg, 1992.
13. B. R. Pamplin, *Tables of Properties of Semiconductors*, CRC Handbook of Chemistry and Physics, Volume 68, pp 102 - 105, 1987-1988.
14. Martin J. Weber, Editor, *CRC Handbook of Laser Science and Technology*, Vol III, Part 1, CRC Press, Inc., Boca Raton, Florida, 1986.
15. G. D. Boyd, H. Kasper, and J. H. McFee, *IEEE J. of Q. Electr.* **QE-7**, 563 (1971).
16. C. K. N. Patel, *Phys. Rev. Lett.* **16**, 613 (1966).
17. J. H. McFee, G. D. Boyd, and P. H. Schmidt, *Appl. Phys. Lett.* **17**, 57 (1970).
18. G. D. Boyd, E. Buehler, and F. G. Storz, *Appl. Phys. Lett.* **18**, 301 (1971).
19. B. F. Levine and C. G. Bethea, *Appl. Phys. Lett.* **20**, 272 (1972).

20. W. B. Gandrud, G. D. Boyd, J. H. McFee, and F. H. Wehmeier, *Appl. Phys. Lett.* **16**, 59 (1970).
21. R. C. Miller and W. A. Nordland, *Phys. Rev. B* **2**, 4896 (1970).
22. Marvin. J. Weber, Editor, *CRC Handbook of Laser Science and Technology*, Vol. IV, Part 2, CRC Press, Boca Raton, Florida, 1986.
23. N. M. Ravindra and V. K. Srivastava, *Infrared Phys.* **19**, 605 (1979).
24. Lockheed Sanders-Laser & Electro-optics, Technical Data Sheet (Zinc Germanium Phosphide), Nov 1, 1993.
25. O. Madelung and M. Schulz, Editors, *Landolt-Bornstein: Numerical Data and Functional Relationships in Science and Technology; Group III: Crystal and Solid State Physics: Semiconductors*, Volume 22, subvol. a, Springer-Verlag, New York, 1987.
26. N. M. Ravindra and V. K. Srivastava, *Infrared Phys.* **19**, 603 (1979).
27. T. S. Moss, *Proc. Phys. Soc.* **B63**, 167 (1950).
28. J. F. Nye, *Physical Properties of Crystals*, Oxford Science Publications, New York, 1989.
29. J. C. Phillips, *Phys. Rev. Lett.* **20**, 550 (1968).
30. J. A. Van Vechten, *Phys. Rev.* **182**, 891 (1969); *Phys. Rev.* **187**, 1007 (1969).
31. R. A. Soref, *J. Appl. Phys.* **72**, 626 (1992).
32. Robert C. Miller, *Appl. Phys. Lett.* **5**, 17 (1995).
33. C. Flytzanis, in *Nonlinear Optics of Organics and Semiconductors*, T. Kobayashi editor, Springer Proceedings in Physics, Vol. 36, Springer-Verlag, Heidelberg, 1989, page 14.
34. Chr. Flytzanis and J. Ducuing, *Phys. Rev.* **178**, 1218 (1969).
35. B. F. Levine, *Phys. Rev. B* **7**, 2600 (1973).
- 37 Zachary H. Levine and Douglas C. Allan, *Phys. Rev. Lett.* **66**, 41 (1991).
38. Hua Zhong, Zachary H. Levine, Douglas, C. Allan, and John W. Wilkins, *Phys. Rev. Lett.* **69**, 379 (1992).
36. M. Sheik-Bahae, D. C. Hutchings, D. J. Hagan, and E. W. van Stryland, *IEEE J. Quantum*

Electron. **27**, 1296 (1991).

39. A. M. Prokhorov and Yu S. Kuz'minov, *Ferroelectric Crystals for Laser Radiation Control*, Adam Hilger, Bristol, Philadelphia, and New York, 1990.

40. J. L. Shay and J. H. Wernick, *Ternary Chalcopyrite Semiconductors: Growth, Electronic Properties, and Applications*, Pergamon, New York, 1975.

41. S. H. Wei and Alex Zunger, *Appl. Phys. Lett.* **56**, 662 (1990).

42. V. E. Stenger, P. B. Kosel, S. M. Hegde, and M. C. Ohmer, Proceedings of SOTAPOCS XVIII, **93-27**, 75, Electrochemical Society, 1993.

43. T. Bell, J. L. Shay, and H. M. Kasper, *Phys. Rev. B* **9**, 5203 (1974).

44. S. I. Radautsan and I. M. Tiginyanu, *Jpn. J. Appl. Phys.* **32**, Suppl 32-3, 5 (1993).

45. U. von Alpen, J. C. Doukhan, B. Escaig, and P. Grosse, *Phys. Status Solidi. B* **55**, 667 (1973).

46. L. S. Dubinskaya, A. D. Galetskaya, and I. I. Farbshtein, *Sov. Phys. Solid State* **24**, 1536 (1983).

47. Joseph J. Loferski, *Phys. Rev.* **93**, 707 (1954).

48. J. Stuke and H. Keller, *Phys. Status Solidi* **7**, 189 (1964).

49. John W. Wilkins, (private communication).

Table 1. Data used to plot $\chi^{(2)}$ against band gap. Sources of the data are given in the references listed at the bottom of the table. δ_{ij} = Miller's delta; Index = index of refraction. Units are Gap in eV, χ in pm/V, FOM in (pm/V)² and δ_{ij} in m²/C.

	Compound	Ref No.	Gap	$\chi^{(2)}$	FOM	Index	δ_{ij}
1	InSb	a,b	0.23	3268.0	43322.43	3.95	0.056
2	Te	c	0.33	1300.0	3834.71	4.794	0.007
3	GeSn	a,p,q	0.36	2308.0	14614.17	4.5	0.02
4	InAs	a,d	0.36	838.0	4388.84	3.42	0.033
5	CdGeAs ₂	c,e,f	0.57	820.0	3821.59	3.5	0.029
6	GaSb	d	0.72	1256.0	7785.99	3.7	0.028
7	SiSn	a,p,q	0.84	1010.0	4138.01	3.95	0.02
8	SiGe	a,p,q	0.9	674.0	2224.02	3.71	0.02
9	SnC	a,p,q	1.2	556.0	1656.46	3.6	0.02
10	AgInSe ₂	c,e,g,h	1.2	100.0	135.87	2.6	0.031
11	InSe	a	1.25	200.0	131.19	4.2	-
12	InP	d	1.35	287.0	505.86	3.4	0.008
13	GaAs	b,d	1.4	270.0	521.22	3.27	0.011
14	CdTe	a,c,i	1.5	336.0	1551.50	2.63	0.077
15	CuInS ₂	c,e,j,k	1.53	19.2	5.43	2.6	0.007
16	CuGaSe ₂	c,e,h,j,k	1.7	70.0	60.87	2.7	0.020
17	Se	b,c	1.7	159.2	344.36	2.64	0.042
18	CdGeP ₂	c,e,f	1.72	320.0	788.62	3.2	0.025
19	ZnSiAs ₂	c,e,f	1.74	180.0	244.89	3.2	0.016
20	AgGaSe ₂	c,e,g,h,k	1.8	95.0	126.90	2.6	0.030
21	CdSe	c	1.8	104.0	183.87	2.5	0.047
22	Ag ₃ SbS ₃	c	1.93	28.0	9.53	2.7	0.006
23	Ag ₃ AsS ₃	a	2	50.0	31.75	2.7	0.012

24	GaSe	c	2.021	128.0	186.59	2.8	0.029
25	ZnGeP2	c,e,f	2.05	150.0	185.21	3.1	0.020
26	HgS	b	2.1	100.0	142.24	2.6	0.029
27	GeC	a,p,q	2.1	76.0	75.02	2.68	0.02
28	AgAsS2	a	2.14	50.0	40.00	2.5	0.022
29	b-SiC	a,p,q	2.26	60.0	51.80	2.59	0.005
30	GaP	c,d,m	2.3	200.0	335.67	3.1	0.020
31	ZnTe	a,c,i	2.3	184.4	431.89	2.7	0.043
32	CuGaS2	c,e,g, h,j,k	2.43	22.0	7.93	2.5	0.011
33	CdS	c	2.485	88.0	181.82	2.2	0.071
34	GaS	a	2.5	279.0	988.68	2.7	-
35	map	l	2.6	12.6	11.76	1.5	-
36	AgGaS2	c,g,h,k	2.638	28.0	14.18	2.4	0.022
37	ZnSe	c,m	2.7	156.8	444.63	2.4	0.077
38	AgI	c	2.8	20.0	5.50	2.6	0.021
39	CuBr	a	2.91	16.0	8.00	2.0	0.033
40	CuI	a	2.95	16.0	5.26	2.3	0.017
41	pom	l	3	6.0	2.20	1.6	-
42	CdGa2S4	a	3.05	50.0	51.37	2.3	0.030
43	CuCl	a	3.17	14.0	7.14	1.9	0.043
44	ZnO	a,b,c	3.3	3.6	0.44	2.0	0.008
45	ZnS	c	3.9	61.2	76.96	2.3	0.066
46	LiIO3	b	4	11.1	2.67	2.3	-
47	LiNbO3	b	4	10.9	4.40	1.9	0.004
48	urea	l	5.9	2.0	0.24	1.6	-
49	SiC	n	6	17.2	3.93	2.7	-

50	AlN	a	6.2	7.7	1.85	2.0	-
51	BBO	l	6.3	1.2	0.09	1.6	-
52	KDP	o	7	0.9	0.06	1.5	0.030
53	SiO ₂	b	8.4	0.8	0.04	1.5	0.015

All $\chi^{(2)}$ and Miller δ data, except IV-IV compounds, are from *the CRC Handbook on Laser Science and Technology, Vol. III*, Ed. Martin J. Weber, CRC Press, Boca Raton, FL, 1986.

a. Editors: O. Madelung and M. Schulz, *Landolt-Bornstein: Numerical Data and Functional Relationships in Science and Technology; Group III: Crystal and Solid State Physics: Semiconductors*, Volume 22, subvol. a, Springer-Verlag, New York, 1987.

b. R. C. Miller and W. A. Nordland, *Phys. Rev. B* **2**, 4896 (1970).

c. V.G. Dmitriev, G.G. Gurzadyan, and D.N. Nikogosyan, *Handbook of Nonlinear Optical Crystals*, Springer Series in Optical Sciences, Vol. 64, Springer-Verlag Berlin Heidelberg, 1991.

d. Lockheed Sanders-Laser & Electro-optics, Technical Data Sheet (Zinc Germanium Phosphide), Nov 1, 1993.

e. M. Mondal, K. P. Ghatak, and A. K. Das, *Acta Physica Hungarica* **65**, 43 (1989).

f. H. Hahn and B. Wellmann, *Naturwissenschaften* **54**, 42 (1967).

g. H. Y. Ueng, and H. L. Hwang, *Mat. Sci. and Eng.* **B12**, 261 (1992).

h. M. Mondal, S. Banik, and K. P. Ghatak, *J. Low Temp. Phys.* **74**, 423 (1989).

i. N. M. Ravindra and V. K. Srivastava, *Infrared Phys.* **19**, 603 (1979).

j. J. E. Jaffe and A. Zunger, *Phys. Rev. B* **29**, 1882 (1984).

k. J. L. Zyskind and A. Srivastava, *J. Crys. Growth* **81**, 530 (1987).

l. B. R. Pamplin, T. Kiyosawa, and K. Masumoto, *Prog. Crystal. Growth Charact.* **1**, 331 (1979).

m. N. M. Ravindra and V. K. Srivastava, *Infrared Phys.* **19**, 605 (1979).

- n. Elgene R. Nichols, John C. Corbin Jr., Vincent L. Donlan, Technical Report AFAL-TR-74-161, pp 61-63, July 1974. Available from NTIS.
- o. P. Villars and L. D. Calvert, *Pearson's Handbook of Crystallographic Data for Intermetallic Phases*; Vols. I, II, III, American Society for Metals, Metals Park, Ohio 44073, 1985 (first printing).
- p. R. Soref, *Appl. Opt.* **31**, 4627 (1992).
- q. R. Soref, *J. Appl. Phys.* **72**, 626 (1992).

Table 2. Summary of Numerical Fit Equations for $\chi^{(2)}$ (pm/V) and for figure of merit (FOM) (pm/V)² for E = 0-8 eV (full gap range), 0-1 eV (narrow gap range), and 1-8 eV (wide gap range).

Full Gap Range:	$\chi^{(2)} = 291E^{-1.92}$	correlation coef = 0.9
Narrow Gap Range:	$\chi^{(2)} = 663E^{-.89}$	correlation coef = .88
Wide Gap Range:	$\chi^{(2)} = 510E^{-2.6}$	correlation coef. = 0.78
Full Gap Range:	FOM = 666E^{-3.0}	correlation coef. = 0.86
Narrow Gap Range:	FOM = 2324E^{-1.4}	correlation coef. = 0.85
Wide Gap Range:	FOM = 1760E^{-4.1}	correlation coef. = 0.76

Table 3. Predicted $\chi^{(2)}$ (pm/V) and FOM (pm/V)² values compared with actual values for the three line fits for compounds representative of narrow, mid, and wide energy gap values.

$\chi^{(2)}$:

E	Full	Narrow	Wide	Actual	Compound
0.23	4.91E+03	<u>2.45E+03</u>	2.26E+04	<u>3.27E+03</u>	InSb (narrow)
1.4	1.52E+02	4.91E+02	<u>2.14E+02</u>	<u>1.80E+02</u>	GaAs (mid)
7.0	6.88E+00	1.17E+02	<u>3.37E+00</u>	<u>1.00E+00</u>	KDP (wide)

FOM:

E	Full	Narrow	Wide	Actual	Compound
0.23	5.61E+04	<u>1.84E+04</u>	7.65E+05	<u>4.33E+04</u>	InSb (narrow)
1.4	2.41E+02	1.45E+03	<u>4.37E+02</u>	<u>2.32E+02</u>	GaAs (mid)
7.0	1.88E+00	1.51E+02	<u>5.63E-01</u>	<u>1.00E-01</u>	KDP (wide)

Table 4. Comparison of the calculated and literature values of $\chi^{(2)}$. Calculated values from equations in Table 2.

Compound	E (eV)	$\chi^{(2)}$ -Est. (pm/V)	$\chi^{(2)}$ -Exp** (pm/V)	Rel. $\chi^{(2)}$ Calculated	Exp	Estimated/ Exp Value
GaInP ₂	1.7	130	-	-	-	-
GaAs	1.4	214	180	-	-	1.19
AgGaS ₂	2.73	38.3	28	1.00	1.00	1.37
AgGaSe ₂	1.83	107	95	2.79	3.39	1.13
AgGaTe ₂	1.356	233	(170)*	6.08	-	-
HgGa ₂ S ₄	2.79	36.2	53.6, 70.4	1.00	-	0.56, 0.42
HgGa ₂ Se ₄	2.1	75.3	-	2.08	-	-
HgIn ₂ Se ₄	1.45	196	-	5.41	-	-
Se	1.7	130	159	1.00	1.00	0.82
Te _{.286} Se _{.714}	1	510	(624)*	3.92	-	-
Te	0.33	1780	1300	13.69	8.18	1.37
ZnGeP ₂	2	85.4	150	1.00	1.00	0.57
CdGeAs ₂	0.57	1090	820	12.76	5.47	1.33

**Reference 11

*Calculated using ratio, e.g., 233/38.3 = 6.08; 28*6.08 = 170.

Table 5. Comparison of calculated and literature values for the Figure of Merit.
Calculated values from equations in Table 2.

Compound	E (eV)	FOM-Calc (p m/V) ²	FOM-Exp (p m/V) ²	Relative FOM Calculated	FOM Exp.	Estimated/ Exp Value
GaInP ₂	1.7	196	-	-	-	-
GaAs	1.4	437	232	-	-	1.88
AgGaS ₂	2.73	27.6	23.4	1.00	1	1.18
AgGaSe ₂	1.83	144	127	5.22	5.43	1.13
AgGaTe ₂	1.356	498	(422)*	18.04	-	-
HgGa ₂ S ₄	2.79	25.2	-	1.00	-	-
HgGa ₂ Se ₄	2.1	81.7	-	3.24	-	-
HgIn ₂ Se ₄	1.45	378	-	15.00	-	-
Se	1.7	196	511	1.00	1	0.38
Te _{.286} Se _{.714}	1	1760	(4589)*	8.98	-	-
Te	0.33	11000	10,048	56.12	19.66	1.09
ZnGeP ₂	2	99.9	185	1.00	1	0.54
CdGeAs ₂	0.57	5120	3822	51.25	20.66	1.34

*Calculated using ratio

Table 6. Power-law scaling summary, where m is the bandgap power dependence.

FOM	m	Bandgap Range (eV)	Reference
	$\chi^{(2)}$		
3.0	1.9	8 - 0	this work
4.1	2.6	8 - 1	this work
1.4	0.9	1 - 0	this work
6	3	1.4 - 2.45	"nearly" <i>ab initio</i>, refs. 37, 38

Figure Captions:

Figure 1. Plot of the second order nonlinear coefficient, $\chi^{(2)}$, versus bandgap for a number of chalcopyrites and selected other types of compounds. See Table 1 for specific data. The “nearly” *ab initio* results (dashed line) and values calculated using Miller’s empirical rule, as given by equation 7, are plotted for comparison. open boxes: narrow gap; open circles: wide gap; x: Miller’s rule; filled diamonds: *ab initio* calculated values; the solid lines are fits for each range; the dotted line is the fit for *ab initio* values.

Figure 2. Plot of the figure of merit (FOM) versus bandgap for a number of chalcopyrites and selected other types of compounds. The “nearly” *ab initio* result (dashed line) is shown for comparison. Open boxes: narrow gap; open circles: wide gap; filled diamonds: *ab initio* values; solid lines: fits for two ranges; dotted line: fit for *ab initio* values.

